Soft Matter

Accepted Manuscript

ROYAL SOCIETY OF CHEMISTRY

www.rsc.org/softmatter

For Table of Contents Use Only

From Multi-responsive Tri- and Diblock Copolymers to Diblock-Copolymer-Decorated Gold Nanoparticles: Effect of Architecture on Micellization Behaviors in Aqueous Solutions

Lichun Song, Hui Sun, Xiaolu Chen, Xia Han*, Honglai Liu

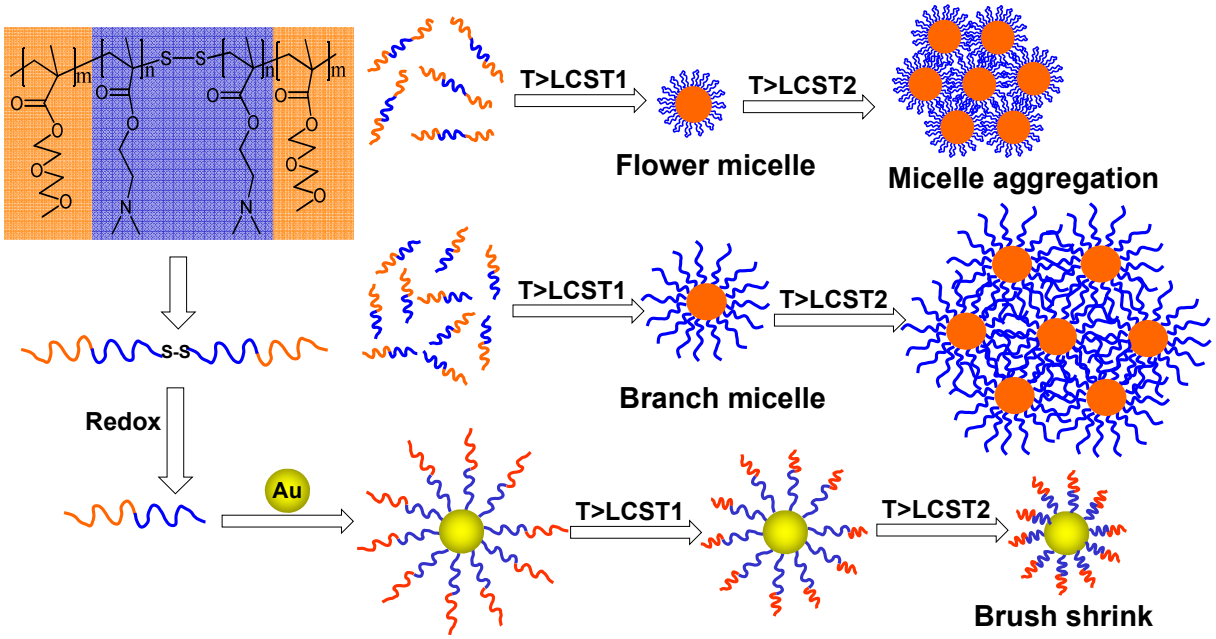

ABSTRACT: This work reports on the aqueous stimuli-responsive behaviors of an ABA triblock copolymer, a BAB triblock copolymer, an AB diblock copolymer and citrate-based gold nanoparticles decorated with AB diblock copolymers (where A is the pH- and thermo-responsive poly[N,N-(dimethylamino) ethyl methacrylate] (PDMAEMA) and B is the thermo-responsive poly[2-(2-methoxyethoxy) ethyl methacrylate] ($PMEO_2MA$)). The symmetric triblock polymers were synthesized via sequential atom transfer radical polymerization (ATRP) using a disulfide-functionalized initiator. Subsequently, the thiol-ended diblock copolymers were facilely obtained by reducing these triblock copolymers and were grafted onto gold nanoparticle (AuNP) surfaces via ligand exchange to yield stimuli-sensitive gold nanoparticles (Au@AB and Au@BA). The ABA and BAB triblock copolymers exhibited two-step thermo-induced aggregation behavior in water at a pH near the isoelectric point (IEP), which

* Corresponding author: Tel: +86-21-64251942; Fax: +86-21-64252922; E-mail: xhan@ecust.edu.cn

resulted in the formation of micelles after the first lower critical solution temperature (LCST) and large aggregates consisting of clustered micelles above the second LCST transition. The significant difference between the micelle sizes of the ABA and BAB copolymers, such that the micelle size of the BAB copolymer was smaller than that of the ABA copolymer although both had a similar unit composition, suggests a distinction between the micelle structures. The "branch" and "flower-like" micelles that formed in the ABA and BAB aqueous solutions, respectively, ultimately governed the phase transition behaviors. The AB diblock copolymer exhibited similar micellization behavior and a micelle size roughly similar to that of the ABA triblock copolymer, although the chain length of the AB copolymer is only half that of the ABA copolymer. Both Au@PDMAEMA-PMEO$_2$MA and Au@PMEO$_2$MA-PDMAEMA showed similar dual LCST behaviors and pH-responsive behaviors in aqueous solutions without the addition of salt. A significant difference was observed between the two types of hybrid AuNPs in salty solutions, in which only the Au@PDMAEMA-PMEO$_2$MA system exhibited thermo-induced aggregation behavior. These hybrid nanoparticles can be used as phase transfer reagents. Additionally, AuNPs capped with PDMAEMA-PMEO$_2$MA diblock copolymer can spontaneously transfer across a water-toluene interface.

KEYWORDS: Multi-responsive copolymer · micellization behaviors · gold nanoparticle · polymer brush · responsive nanoparticle

From Multi-responsive Tri- and Diblock Copolymers to Diblock-Copolymer-Decorated Gold Nanoparticles: Effect of Architecture on Micellization Behaviors in Aqueous Solutions

Lichun Song, Hui Sun, Xiaolu Chen, Xia Han*, Honglai Liu

Key Laboratory for Advanced Materials and Department of Chemistry, East China University of Science and Technology, Shanghai 200237, China

INTRODUCTION

Stimuli-responsive water-soluble polymers typically exhibit reversible or irreversible changes in their chemical structures and/or physical properties in response to specific signal inputs, such as pH, temperature, ionic strength, or light irradiation.[1] Over the past two decades, significant advances have been achieved in the field of stimuli-responsive polymers, and such efforts still attract considerable attention because of their potential applications in many fields, such as environmental protection, drug delivery systems, sensors, paints, membranes, and antibacterial materials.[2-5] Block copolymers can self-assemble into various aggregates, of which the most common form is spherical micelles with a hydrophobic insoluble core and a hydrophilic shell.[6] Many studies have revealed that the composition, molecular architecture, molecular weight, and solution concentration of these copolymers influence their micellar properties.[7] Recently, it was found that the block copolymer architecture also plays an important role in determining micellar properties,[8] especially for stimuli-responsive block copolymers in which hydrophobic/hydrophilic transitions occur in aqueous solution, leading to self-assemblies with different structures that depend on the properties of the blocks and the block architectures.[9-11] The effect of the architecture on the micellization behaviors of copolymers in aqueous solutions have been studied using thermo-responsive polymers based on n-butyl methacrylate (BuMA), which is non-ionic and hydrophobic; 2-(dimethylamino)ethyl methacrylate (DMAEMA), which is ionizable, hydrophilic and thermo-responsive; and methoxy poly(ethylene glycol) methacrylate (PEGMA), which is non-ionic and hydrophilic. It was found that the polymer composition influenced the cloud points and the pKas and that both the polymer composition and architecture strongly influenced the thermo-responsive behavior of the triblock copolymers in water. Liu et al.[12] compared the thermo-responsive micellization behaviors of ABA and BAB triblock thermo-responsive copolymers (A=N-

* Address correspondence to xhan@ecust.edu.cn

isopropylacrylamide (NIPAAm), B=2-hydroxyethyl methacrylate (HEMA)) and found that the BAB copolymer exhibited a higher transition temperature and a good solubility in water compared with the ABA copolymer of the same composition and concentration; this observation was attributed to their distinct micellar structures. The micelle formation of five poly(2-oxazoline) diblock, triblock and gradient copolymers in water was investigated using fluorescence correlation spectroscopy, and the results showed that the hydrodynamic radii of the aggregates (micelles) depended on the polymer architecture in a characteristic manner.[13]

Recently, the design of core–shell gold nanoparticles (AuNPs) has attracted increasing interest, not only as a means of improving the stability and surface chemistry of the core nanoparticle but also as a method of accessing unique structures, properties and applications by combining the different characteristics of the components.[14,15] Using the "grafting from" or "grafting to" approaches, stimuli-responsive polymers can be grafted onto gold nanoparticles to fabricate hybrid gold nanoparticles with stimuli responsiveness, enhanced colloidal stability, and improved biocompatibility, which are of considerable interest because of the prospective applications of such nanoparticles in phase transfer catalysis, biotechnology, nanotechnology, and drug delivery.[16-19] Homopolymers[20-22] and statistical copolymers[23-26] have been used to fabricate stimuli-responsive gold nanoparticle brushes for application in phase transfer[27-30], antifouling[16], and catalysis[19], among others. However, the use of block copolymers[18,31] for this purpose has the advantage of allowing for the programming of different polymer blocks with specific functions and for quantitative control over the chemical functionality and composition as well as the architectural complexity of the polymer chains on the surfaces of the nanoparticles.[32] Diblock copolymers composed of poly(ethylene oxide) (PEO) and poly(N,N-dimethylaminoethyl methacrylate) (PEO-b-PDMAEMA) tethered to AuNP surfaces can undergo a thermally induced solubility change characterized by either an LCST (with PEO-b-PDMAEMA) or an upper critical solution temperature (UCST) (with quaternized PEO-b-PDMAEMA).[18] Hybrid gold nanoparticles modified with poly(N-isopropylacrylamide)-block-poly(2-succinyloxyethyl methacrylate) (PNIPAM-b-PSEMA) brushes demonstrate reversible pH- and temperature-controlled changes in size and aggregation state in solution.[31] Although progress has been made in the design and preparation of multiple-stimuli-responsive block copolymers, the preparation of stimuli-responsive polymer brush-grafted particles, and the design of stimuli-triggered systems for phase transfer applications, attempts to gain a fundamental understanding of the effect of the block sequence on the responsive behaviors of such systems

and to control their phase transfer behaviors have rarely been explored.[33,34] Additionally, an explanation of whether and to what extent the properties of polymer-coated AuNPs formed through the conjugation of stimuli-responsive particles to gold nanoparticles differ from those of the free polymers is still lacking.[35]

PDMAEMA is a widely studied pH- and thermo-responsive polymer.[36] The tertiary amine groups along its main chain can be charged or uncharged at low or high pH, respectively,[37] which can induce a pH-dependent thermo-responsive behavior in aqueous solution.[38-41] Herein, we report a dual-stimuli-responsive block copolymer system composed of the pH- and thermo-responsive poly[N,N-(dimethylamino) ethyl methacrylate] (PDMAEMA) and the thermo-responsive poly[2-(2-methoxyethoxy) ethyl methacrylate] ($PMEO_2MA$). Triblock copolymers were fabricated by introducing a facile method for the synthesis of block copolymers linked via a disulfide functionality, which offered the possibility of designing a multi-responsive polymeric system by incorporating a temperature-responsive $PMEO_2MA$ block, a pH- and thermo-responsive PDMAEMA block, and a redox-responsive disulfide linker. These copolymers, which were obtained via sequential atom transfer radical polymerization (ATRP), presented tunable double LCSTs that were highly pH dependent. A diblock copolymer with an end terminated with a thiol group was easily obtained by reducing the disulfide linkage to a thiol in the presence of tris(2-carboxyethyl) phosphine hydrochloride (TCEP) and was grafted onto the surfaces of AuNPs via covalent Au−S bonds using the solution ligand exchange approach to form Au@copolymer hybrid nanoparticles. The hybrid nanoparticles possessed enhanced pH-responsive and suppressed thermo-responsive properties compared with those of the free diblock copolymers. More importantly, these materials can be used as reagents for phase transfer from toluene to aqueous solutions that are triggered by the addition of acid or hexane.

RESULTS AND DISCUSSION

Responsive behaviors of ABA and BAB triblock copolymers in aqueous solutions. $PMEO_2MA$ is a thermo-responsive homopolymer that dissolves molecularly at 25 °C in aqueous solution but precipitates above its LCST of approximately 31 °C. By contrast, the solubility and thermo-responsive behavior of the PDMAEMA homopolymer in aqueous solution is dependent on pH (see the Supporting Information). **Figure 1** shows the temperature-dependent transmittance and hydrodynamic diameters of the $PDMAEMA_{46}$-$PMEO_2MA_{68}$-$PDMAEMA_{46}$ (ABA) triblock copolymer in aqueous solutions at different pH values. The triblock copolymer is

molecularly soluble in water at temperatures below 30.0 °C for all pH values investigated, as indicated by the nearly constant transmittance at ~100%. The hydrodynamic diameter (Dh) values of the $PDMAEMA_{46}$-$PMEO_2MA_{68}$-$PDMAEMA_{46}$ copolymer at these temperatures were ~10 nm, suggesting molecularly dissolved polymer chains consistent with the transmittance results. When the temperature was increased to 32 °C, the transmittance decreased gradually to 70% at pH=6.9 and decreased sharply to 0% at pH=9.6. These micellization behaviors were confirmed by the dynamic light scattering (DLS) analysis, in which the Dh was constantly maintained at ~250 nm at pH=6.9 and at 775±10 nm at pH=9.6. At pH=9.0, however, the transmittance exhibited a two-step drop to 0%, indicating different micellization behaviors of the triblock copolymer. The Dh increased to ~250 nm at 32 °C, underwent a slight decrease to 95±5 nm in the following temperature range of 38-56 °C, and subsequently increased monotonically to ~2000 nm at temperatures above 60 °C. It is suggested that the triblock copolymer underwent a two-step aggregation phenomenon in which the collapse of the $PMEO_2MA$ induced branch micelles at the first LCST ($LCST_1$) and these branch micelles then underwent secondary aggregation to form large aggregates due to the dehydration of the micelle shells at the second LCST ($LCST_2$). The decrease of the Dh in the temperature range of 38-56 °C indicates the shrinkage of the highly swollen hydrophilic corona of the spherical micelles.

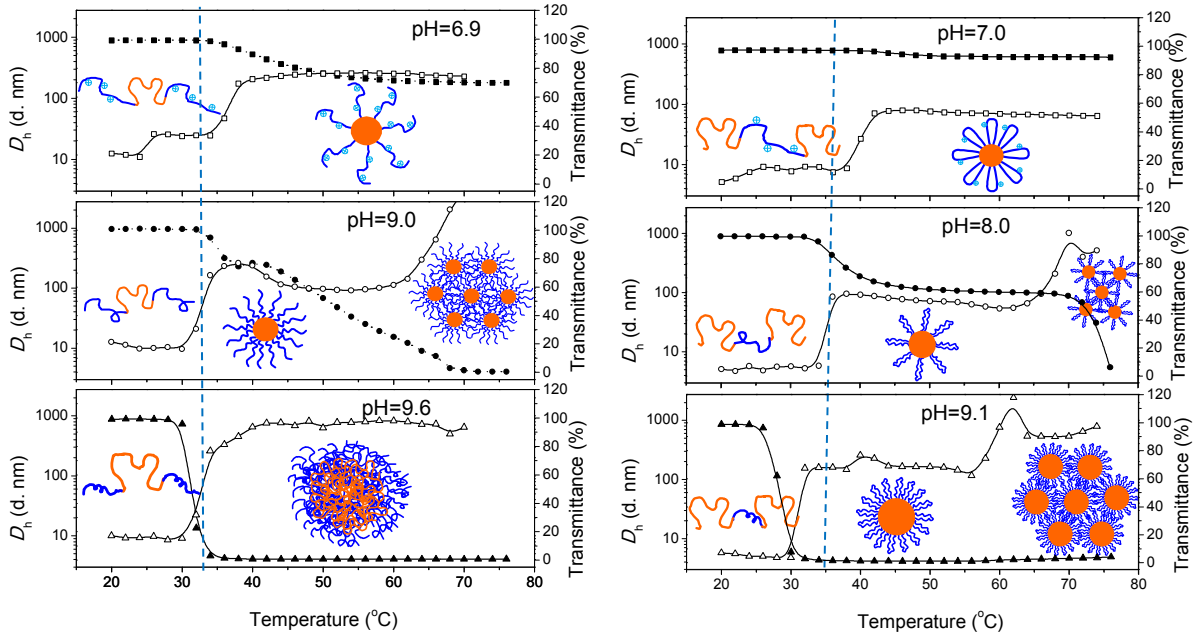

Figure 1. Dynamic light scattering and turbidity measurements in aqueous solutions of block copolymers at different pH values. Left panel: $PDMAEMA_{46}$-$PMEO_2MA_{68}$-$PDMAEMA_{46}$ (ABA). Right panel: $PMEO_2MA_{80}$-$PDMAEMA_{54}$-$PMEO_2MA_{80}$

(BAB). The open symbols represent the hydrodynamic diameters. The solid symbols represent the temperature-dependent transmittance.

Responsive behaviors of the BAB triblock copolymer and AB diblock copolymer in aqueous solutions. The thermo-responsive behavior of the BAB triblock copolymer in aqueous solution exhibited a trend similar to that of the ABA triblock copolymer. However, the micelle size of the BAB copolymer was slightly smaller than that of the ABA copolymer with a similar composition at the same pH. For example, at pH~7.0, the micelle size of the BAB copolymer was approximately 70±5 nm, whereas that of the ABA was approximately ~250 nm. The transmittance of the solutions was well consistent with the DLS results. The difference between the behaviors of the copolymers is attributed to their distinct micellar structures regulated by the triblock copolymer architecture[12]. As schematically illustrated in **Figure 1**, branch micelles with a collapsed $PMEO_2MA$ core and a highly swollen hydrophilic PDMAEMA corona formed in the ABA triblock copolymer. For the BAB triblock copolymer, flower-like micelles formed via temperature-induced micellization, in which the two end $PMEO_2MA$ blocks collapsed to form the inner tight core and the middle PDMAEMA block was composed of the outer corona inserted into the core. Thus, the micelle size of the latter material was slightly smaller and exhibited smaller fluctuations with increasing temperature because of the tight micelle structure.

Relative to the complexity of the architecture of the triblock copolymers, the linear diblock copolymer also underwent temperature-induced micellar assembly but formed only conventional branch micelles, with a hydrophobic $PMEO_2MA$ core and a hydrophilic PDMAEMA corona, rather than flower-like micelles. It is evident from **Figure 2** that the $PMEO_2MA_{80}$-$PDMAEMA_{27}$ diblock copolymer formed micelles with a Dh of ~150 nm, similar to the micelle size of the $PMEO_2MA_{80}$-$PDMAEMA_{54}$-$PMEO_2MA_{80}$ triblock copolymer, with twice the composition units.

It has been demonstrated that the LCST of the BAB copolymer is higher than that of the ABA copolymer at the same solution concentration and sequence composition for the HEMA-NIPAAm-HEMA system[12]. However, our system is a dual-stimuli-responsive system, in which the PDMAEMA is a pH-responsive block. Thus, the pH value is a dominant parameter in determining its stimuli-responsive aggregation behavior. In this case, the effect of the block sequence on the LCST is not significant because of the broader transition temperature range of the

block copolymer. It is worth noting that both the micelle size and the LCST are pH dependent. For all systems studied in this work, the LCST decreases as the pH increases. Specifically, the LCST of a $PMEO_2MA_{80}$-$PDMAEMA_{54}$-$PMEO_2MA_{80}$ solution is approximately 40 °C at pH=7.0, which is higher than that at pH=8.0 (approximately 35 °C) and that at pH=9.1 (approximately 31 °C) because of the lower hydrophilicity of PDMAEMA at higher pH.

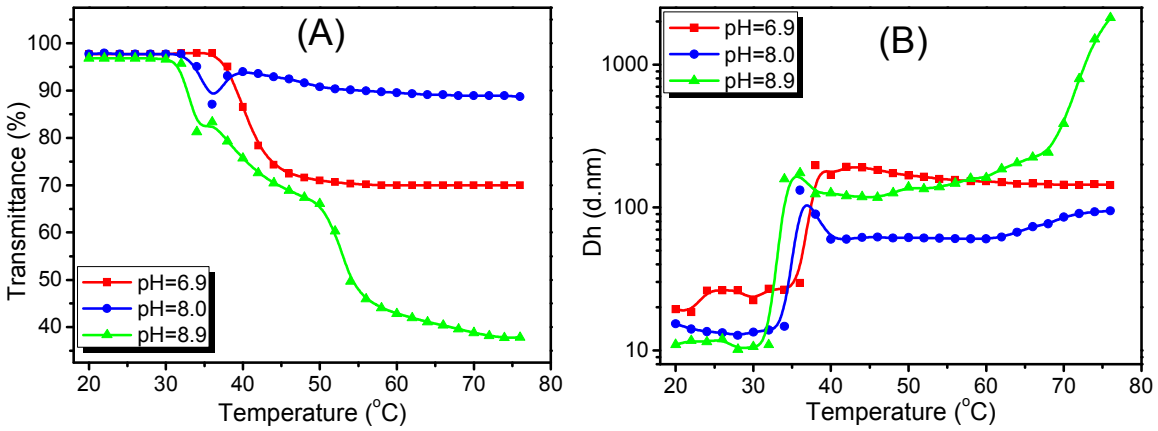

Figure 2. Turbidity measurements (A) and dynamic light scattering measurements (B) in aqueous solutions of the AB diblock copolymer ($PMEO_2MA_{80}$-$PDMAEMA_{27}$) at different pH values.

Responsive behaviors of the Au@AB and Au@BA nanocomposites in aqueous solutions. Highly uniform gold nanoparticles (AuNPs) were synthesized via the established citrate reduction method (reduction of $HAuCl_4$ via boiling with sodium citrate) to yield spherical AuNPs with a diameter close to 15 nm, as observed via transmission electron microscopy (TEM) and DLS (see the Supporting Information). Two diblock copolymers, $PMEO_2MA_{80}$-b-$PDMAEMA_{27}$-SH and $PDMAEMA_{46}$-b-$PMEO_2MA_{34}$-SH, with the PDMAEMA end terminated with a thiol group and with the $PMEO_2MA$ end terminated with a thiol group, respectively, were synthesized by reducing the disulfide of the triblock copolymers to thiol. The two diblock copolymers in aqueous solution were separately mixed with the AuNPs, and the diblock copolymers were grafted onto the surfaces of AuNPs via covalent Au−S bonds using the solution ligand exchange approach. After polymer attachment, the resulting nanocomposite solutions exhibited a slightly broader localized surface plasmon resonance (LSPR) band centered at approximately 533 nm that presented a red shift of ~8 nm compared with the starting AuNPs, thus revealing that each individual particle had been successfully coated without aggregation. This success was further

confirmed by the DLS results, in which, for example, a clear increase of the size distribution peak of the Au@PDMAEMA$_{27}$-b-PMEO$_2$MA$_{80}$ NPs was found compared with that of the starting AuNPs (see the Supporting Information). Additionally, the PDMAEMA-b-PMEO$_2$MA diblock-copolymer-tethered AuNPs could be well dispersed in good solvents for both constituent blocks, e.g., water, THF, chloroform, and toluene (see the Supporting Information).

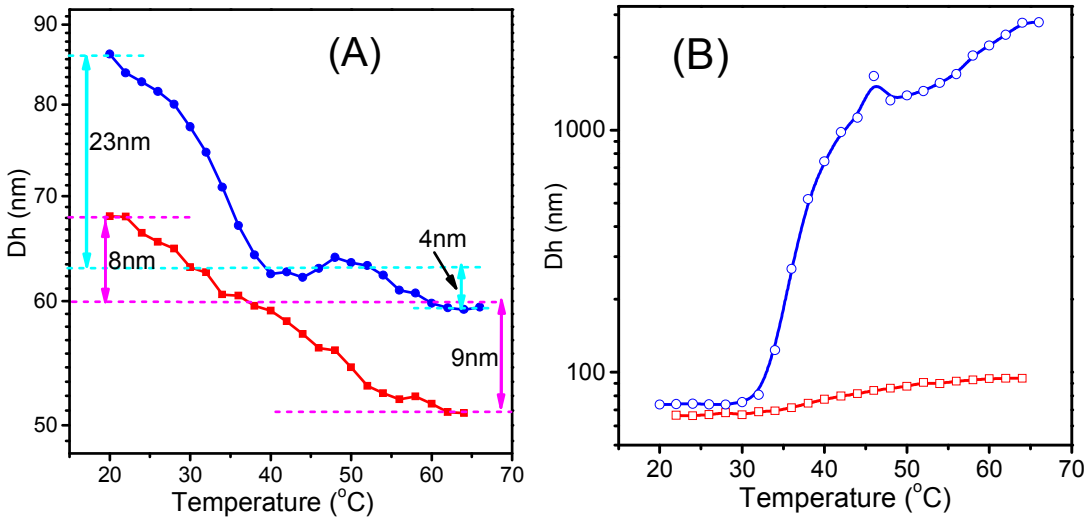

Figure 3. Hydrodynamic diameters of Au@PDMAEMA$_{27}$-b-PMEO$_2$MA$_{80}$ (circles) and Au@PMEO$_2$MA$_{34}$-b-PDMAEMA$_{46}$ (squares) nanocomposites dispersed in water (A) without the addition of NaCl and (B) with the addition of 0.2 mol/L NaCl.

Figure 3 shows the thermo-responsive behavior of the Au@AB and Au@BA nanocomposites in aqueous solutions and in salty solutions. Although the thermo-responsive behavior was not so pronounced as that in the free block copolymer solution, both hybrid systems underwent a two-step decrease in the Dh of the nanoparticles, indicating a two-step shrinkage of the block copolymers tethered to the AuNP cores. The Dh of the Au@PDMAEMA$_{27}$-b-PMEO$_2$MA$_{80}$ NPs decreased rapidly from 86 nm at 20 °C to 63 nm at 42 °C after the first LCST at ~35 °C and then exhibited a milder decrease from 63 nm to 59 nm after the second LCST at ~53 °C. These variations in Dh can be attributed to the conformational changes of the outer PMEO$_2$MA block and the inner PDMAEMA segment, respectively. The Au@PMEO$_2$MA$_{34}$-b-PDMAEMA$_{46}$ system exhibited a similar response behavior but with a suppressed transition tendency, and the decrease in the Dh was approximately 8 nm after the first LCST at 30 °C and approximately 9 nm after the second LCST at 48 °C. It is interesting to note that

the temperature-induced changes in the hydrodynamic diameters of these hybrid AuNPs were much smaller than those of the free copolymers. Accordingly, the LCST values were slightly different and much broader than those determined independently for the two types of homopolymer-decorated AuNPs and for the two free homopolymers in aqueous solution. This observation is attributed to the confinement of the polymer chains at the surface[16] and the incorporation of a hydrophilic component with the polymer.

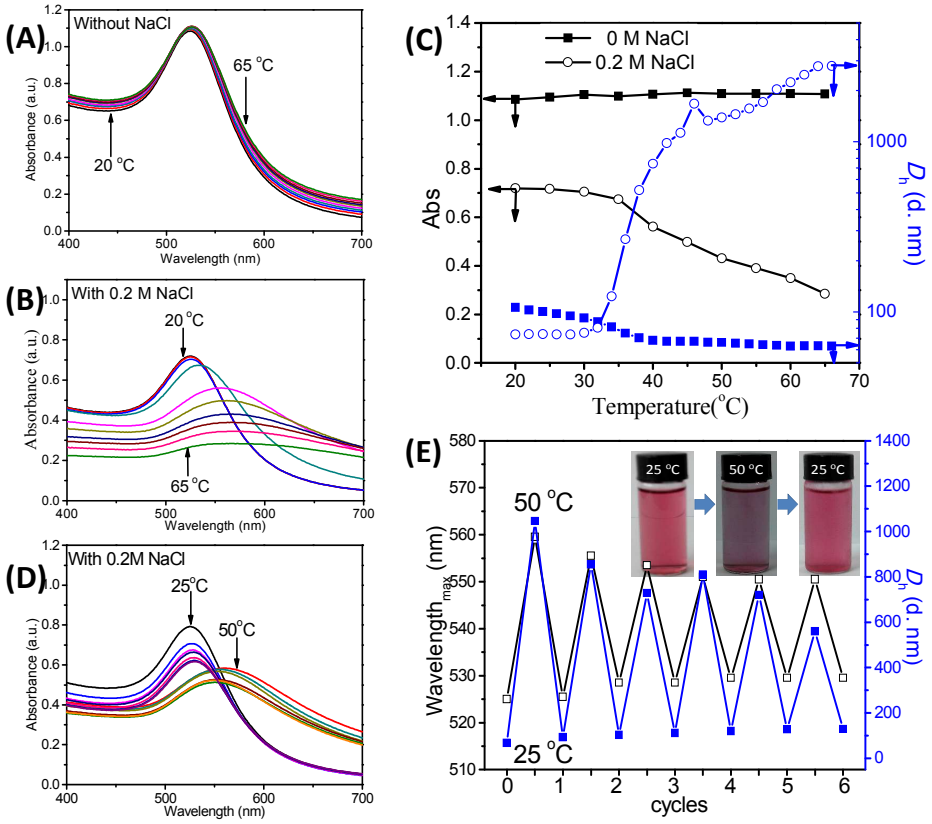

Figure 4. UV–Vis spectra of Au@PDMAEMA$_{27}$-b-PMEO$_2$MA$_{80}$ nanocomposites dispersed in water (A) without the addition of NaCl and (B) with the addition of 0.2 mol/L of NaCl. (C) Absorbance intensity and hydrodynamic diameter (D_h) as functions of temperature. (D) UV–Vis spectra of Au@PDMAEMA$_{27}$-b-PMEO$_2$MA$_{80}$ nanocomposites dispersed in water with the addition of 0.2 mol/L NaCl at 25 °C and 50 °C over several cycles. (E) Maximum wavelength (open black squares) and hydrodynamic diameter (solid blue squares) of Au@PDMAEMA$_{27}$-b-PMEO$_2$MA$_{80}$ nanocomposites over several cycles.

The outcome of this experiment demonstrates the systematic formation of dual-LCST hybrid AuNPs consistent with two different polymer components self-assembled onto the AuNP surfaces. The experiment indicates that the thermo-responsive behaviors of these diblock-copolymer hybrid AuNPs in aqueous solutions are

independent of the sequence of the blocks tethered to the AuNP surfaces. However, a difference in the thermo-responsive behaviors of the hybrid AuNPs is apparent in salty solutions, as shown in **Figure 3B**. A large increase in the Dh of the Au@PDMAEMA$_{27}$-b-PMEO$_2$MA$_{80}$ NPs in an aqueous solution with the addition of 0.2 M NaCl was observed as the temperature was increased to 40 °C, whereas the Dh of the Au@PMEO$_2$MA$_{34}$-b-PDMAEMA$_{46}$ system remained nearly constant. This result is likely attributable to the salting-out theory for polymer solutions.[42] Accordingly, upon the increase in the temperature from 25 °C to 50 °C, the LSPR band of the Au@PDMAEMA$_{27}$-b-PMEO$_2$MA$_{80}$ nanocomposites became much broader and shifted toward higher wavelengths, with a total red shift of ~35 nm. The LSPR band regained its shape and position but became slightly broader when the temperature was again reduced to 25 °C, indicating incomplete disaggregation of the nanoparticles to a minor degree. Correspondingly, the color of the nanocomposites changed from red to purple and then back to red (**Figure 4E** insert). When such heating–cooling cycles were repeated several times, no significant shift in the maximum wavelength was observed during these cycles, but there was a slight decrease in the Dh.

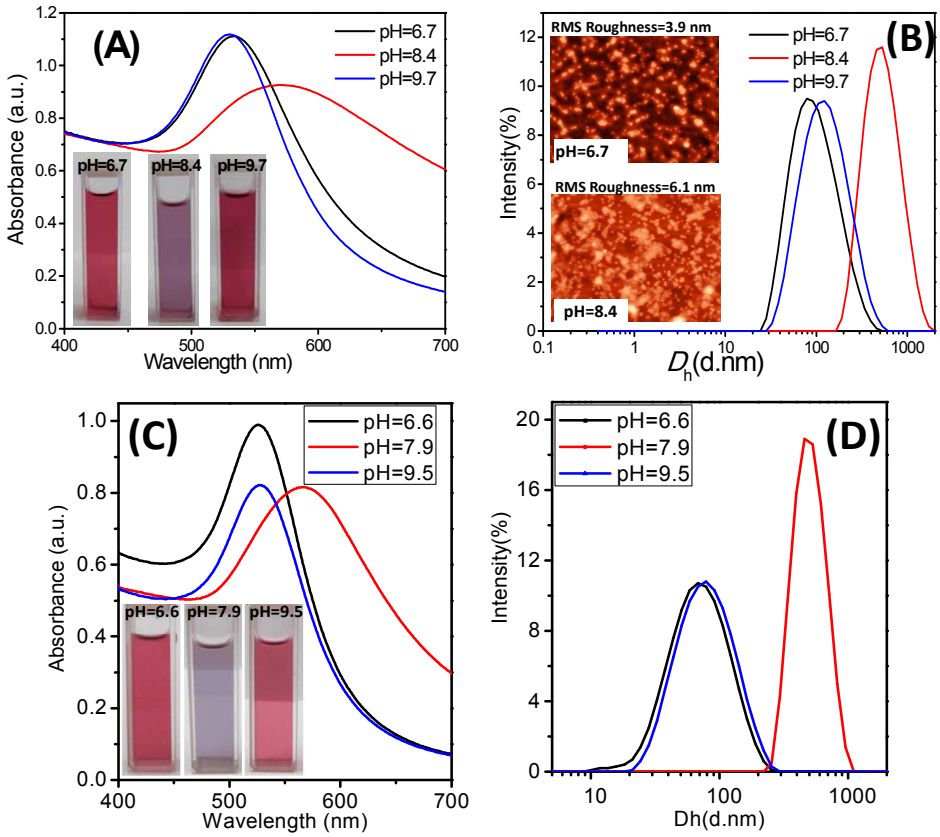

Figure 5. Reversible pH-responsive behavior of AuNPs. (A) UV–Vis spectra of Au@PDMAEMA$_{27}$-PMEO$_2$MA$_{80}$ NPs at

pH=6.7, 8.4, and 9.7. Inset: Representative photograph of Au@PDMAEMA$_{27}$-PMEO$_2$MA$_{80}$ NP dispersions at different pH values. The pH values are displayed on the vials. The NPs were colloidally stable at pH<IEP or pH>IEP and aggregated at pH~IEP, resulting in a color change from deep red to purple and a red shift of the LSPR band of approximately 40 nm. (B) Dh distributions of Au@PDMAEMA$_{27}$-PMEO$_2$MA$_{80}$ NPs at pH=6.7, 8.4, and 9.7. Inset: Representative AFM images of Au@PDMAEMA$_{27}$-PMEO$_2$MA$_{80}$ NP dispersions at different pH values drop-cast onto freshly cleaved mica substrates (3×3 μm^2). At pH=6.7, the Au@PDMAEMA$_{27}$-PMEO$_2$MA$_{80}$ colloidal NPs were well dispersed on the surface, with a small root-mean-square (RMS) roughness of 3.9 nm. At pH~IEP, large aggregates could be observed on the surfaces, with a large RMS roughness of 6.1 nm. (C) UV–Vis spectra, representative photographs and (D) Dh distributions of Au@PMEO$_2$MA$_{34}$-PDMAEMA$_{46}$ NPs at pH=6.6, 7.9, and 9.5.

As previously mentioned, the investigated tri- and diblock copolymers exhibit pH-dependent thermo-responsive properties because the pH-responsive PDMAEMA block has a pKa of ~7.5-8.0.[37,43] Similar to the pure diblock copolymer, both the Au@PDMAEMA$_{27}$-b-PMEO$_2$MA$_{80}$ and Au@PMEO$_2$MA$_{34}$-b-PDMAEMA$_{46}$ NPs were found to be highly pH responsive and to exhibit U-shaped dispersibility as a function of the solution pH, with minima near pH values of ~7.7 and ~8.1, respectively, which are close to the isoelectric point (IEP) of the diblock copolymer (see the Supporting Information). For example, as shown in **Figure 5** for the Au@PDMAEMA$_{27}$-b-PMEO$_2$MA$_{80}$ dispersions, the color of the AuNPs dispersions changed from red to purple and back to red again as the pH of the dispersions was increased from 6.7 (lower than the IEP of the dispersion) to 8.4 (near the IEP of the dispersion) and then to 9.7 (higher than the IEP of the dispersion). Accordingly, UV–Visible (UV–Vis) spectroscopy measurements were used to confirm the reversible nature of the pH-responsive behavior, with an LSPR band maximum at approximately 533 nm at a pH far from the IEP and at approximately 571 nm at a pH near the IEP. The aggregates that formed in the dispersions were characterized using DLS measurements, which confirmed the presence of aggregates with sizes of 510 nm at a pH near the IEP and the presence of highly dispersed nanocomposites with a size of 80-120 nm at pH values far from the IEP, as shown in **Figure 5**. The surface morphologies of the films that were drop-cast from dispersions with different pH values also confirmed the aggregation state at pH=IEP.

Phase transfer behaviors of Au@AB and Au@BA triggered by different stimuli. It was demonstrated that

either a temperature change or a pH change will induce aggregation of AuNPs decorated with the PDMAEMA-b-$PMEO_2MA$ diblock copolymer, resulting in reduced optical transmittance of the solution and a red shift of the LSPR band, primarily as a result of reducing the distances between the surfaces of the AuNPs. Recent reports have described the successful transfer of AuNPs coated with stimuli-responsive polymer brushes, such as random copolymers of PMOEGMA and $PMEO_2MA$[29] or mixed polymer brushes of poly(ethylene glycol) and poly(methyl methacrylate) (PMMA)[27], across oil–water interfaces upon the simple application of an external stimulus. In this work, we used the thermo- and pH-responsive block-copolymer-decorated AuNPs as a phase transfer reagent for the crossing of toluene–water interfaces. **Figure 6** shows the phase transfer behaviors of the hybrid nanocomposites triggered by different stimuli. These hybrid AuNPs dispersed in toluene could be partially transferred into the aqueous phase when hexane was added and the environmental temperature was reduced to 4 °C. The transfer behavior is obviously attributable to the collapse of the PDMAEMA blocks when the environment changes from a good solvent (toluene) to a non-solvent (hexane). Similarly, when a small amount of acid or alkali was added, after shaking, the hybrid AuNPs transferred from the toluene to the aqueous phase at 4 °C upon a change in pH because the hybrid AuNPs were colloidally stable and well dispersed when the pH was from the IEP. Interestingly, both the solvent-triggered and pH-triggered phase transfer behaviors of the hybrid nanoparticles proceeded rapidly, within 1 min at temperatures below 5 °C under gentle shaking, similar to the results previously reported by Wang's group.[23,29]

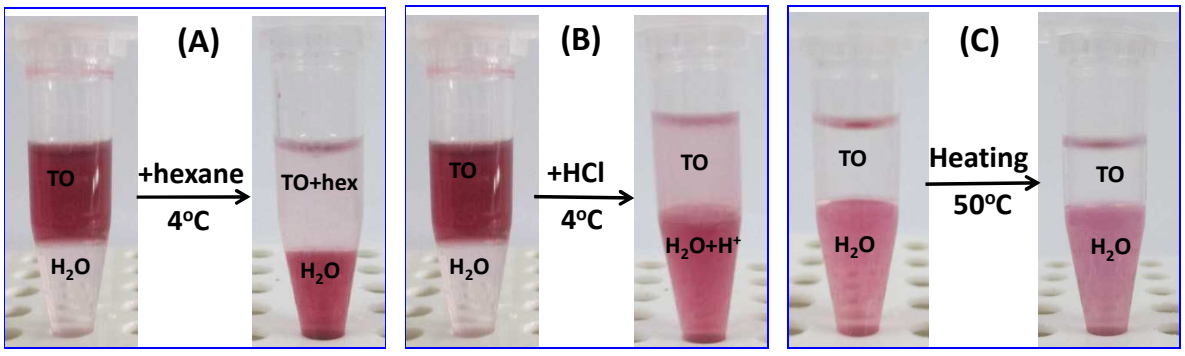

Figure 6. Photographs of the phase transfer process for the Au@PDMAEMA-b-$PMEO_2MA$ system: (A) solvent-triggered NP transfer from toluene to the aqueous phase at 4 °C after shaking, (B) acid-triggered NP transfer from toluene to the aqueous phase at 4 °C after shaking, and (C) retention of NPs in the aqueous phase (0.2 M NaCl) upon heating to 50 °C after shaking.

Surprisingly, temperature alone did not cause the phase transfer of the nanocomposites from the aqueous phase to the toluene phase, even when a salty aqueous phase with 0.2 M NaCl was used. Because of the thermo-responsive aggregation behavior of the Au@PDMAEMA$_{27}$-b-PMEO$_2$MA$_{80}$ NPs in a salty aqueous solution, it was expected that upon a change in temperature, the outer PMEO$_2$MA shells would undergo a hydrophilic-to-hydrophobic transition on the NP surfaces, thereby causing large aggregates of the nanocomposites to form, which would increase the probability for the nanocomposites to cross the water/toluene interface. The fact that this was not observed to occur can be attributed to the difference in stimuli response between free PDMAEMA-b-PMEO$_2$MA copolymers and copolymer-tethered AuNPs; the tethered copolymers cannot alter their conformations as freely as can the free copolymers in solution. It is evident that the phase transfer of the hybrid AuNPs is more sensitive to the pH and the solvent than to the temperature of the surrounding media. Similar phase transfer behaviors of the Au@PMEO$_2$MA$_{34}$-PDMAEMA$_{46}$ NPs were also observed (see the Supporting Information).

CONCLUSIONS

Triblock polymers, a diblock copolymer and diblock-copolymer-decorated gold nanoparticles (AuNPs) based on one hydrophilic and pH- and thermo-responsive monomer (A=PDMAEMA block) and another thermo-responsive monomer (B=PMEO$_2$MA block) were successfully synthesized via sequential atom transfer radical polymerization (ATRP) using a disulfide functionalized initiator, reducing the disulfide to cleave the triblock copolymer, and ligand exchanging the thiol-terminated diblock copolymers to graft them onto AuNPs. The polymer architecture was found to have a significant effect on the thermo-responsive behaviors but not on the pH-responsive behaviors of these polymers in aqueous solutions, i.e., all isoelectric points (IEPs) were similar. The micelle size of the ABA copolymer was found to be larger than that of the BAB copolymer, which has a similar unit composition, but roughly similar to that of the AB copolymer, which has half the chain length of the BAB copolymer, because of the “branch” micelles that form in the ABA and AB solutions and the “flower-like” micelles that form in the BAB aqueous solutions. When block copolymer chains are immobilized onto AuNPs, the sequence and properties of the blocks will affect the stimuli-responsive phase transition from hydrophilic to hydrophobic behavior and will therefore subsequently affect the applications of the nanocomposites. Similar dual-LCST behaviors were observed for both Au@PDMAEMA$_{27}$-b-PMEO$_2$MA$_{80}$ and Au@PMEO$_2$MA$_{34}$-b-

$PDMAEMA_{46}$ nanocomposites in aqueous solutions without the addition of salt, whereas different aggregation behaviors were evident in salty aqueous solutions, in which large aggregates formed only in the Au@$PDMAEMA_{27}$-b-$PMEO_2MA_{80}$ system because of the effect of the sequence of the tethered block copolymer. No significant difference was observed in the reversible pH-responsive behaviors of the Au@AB and Au@BA systems in aqueous solutions because of the independence of the pH-responsive behavior with respect to the block sequence. Subsequently, it was demonstrated that phase transfer of the Au@AB and Au@BA nanocomposites from toluene to the aqueous phase at 4 °C after shaking could be obtained by means of solvent-triggered and pH-triggered changes in dispersity change but not by means of a temperature-triggered driving force.

EXPERIMENTAL SECTION

Materials. The 2-hydroxyethyl disulfide, 2-bromoisobutyryl bromide, triethylamine (TEA), 2-(dimethylamino) ethyl methacrylate (DMAEMA) and di(ethylene glycol) methyl ether methacrylate (MEO_2MA) that were used in this study were purified by passing them through a basic aluminum oxide column prior to use. Copper (I) bromide (Cu^1Br) was washed in acetic acid and ethanol and then dried in a vacuum oven. Tetrahydrofuran (THF, 99%) was refluxed with sodium in the presence of a small amount of benzophenone. (N,N,N′,N″,N″-pentamethyldiethylenetriamine) (PMDETA) (TCI, 98%), ethyl acetate, n-hexane, anhydrous diethyl ether and dichloromethane were used as received.

Synthesis of the ATRP Initiator. The 2, 2'-dithiobis [1-(2-bromo-2-methyl-propionyloxy)] ethane (DTBE) was prepared via acrylation of bis(2-hydroethyl) disulfide[27]. In a typical run, 2-bromoisobutyryl bromide (3.72 mL) was added dropwise to a mixture of disulfide (1.56 mL) and triethylamine (8 mL) in dichloromethane (150 mL) at 0 °C. The solution was stirred at 0 °C for 1 h and then at room temperature for another 2 h. After the precipitates were filtered off, the organic phase was extracted using a 2 N Na_2CO_3 solution saturated with NH_4Cl to remove the excess bromides. The mixture was purified via column chromatography using a mixture of petroleum ether and AcOEt as an eluent to afford DTBE. ^{1}H-NMR (300 MHz, $CDCl_3$) δ: 1.87 (s, 12H, $-CH_3$), 2.92 (t, 4H, J=4.8 Hz, $-SCH_2$), 4.38 (t, 4H, J=4.8 Hz, $-OCH_2$). ^{13}C-NMR (300 MHz, $CDCl_3$) δ: 30.73 ($-CH_3$), 36.73 ($-SCH_2$), 55.52 ($-C(CH_3)_2$), 63.53 ($-OCH_2$), 171.49 (C=O).

Synthesis of the Macroinitiator. The PDMAEMA homopolymer was synthesized using a typical atom

transfer radical polymerization (ATRP) technique. DMAEMA (13.5 mL), PMDETA (185 μL) and disulfide-functionalized DTBE (0.345 g) dissolved in ethyl acetate (20 mL) were placed in a 50-mL Schlenk flask. CuBr (115 mg) was added to the mixture, which was degassed in three freeze–pump–thaw cycles. The flask was placed in an oil bath whose temperature was maintained at 40 °C for 12 h. The reaction was terminated by diluting the mixture with THF and passing it through a neutral alumina column to remove residual CuBr. After the evaporation of excess THF, the mixture was precipitated in cold n-hexane three times to remove unreacted monomers and other impurities. The PDMAEMA homopolymer was obtained after vacuum drying. The $PMEO_2MA$ homopolymer was prepared following the same procedure just by precipitating in cold diethyl ether for three times to remove unreacted monomers and other impurities.

Synthesis of $PMEO_2MA$-b-PDMAEMA-b-$PMEO_2MA$. The $PMEO_2MA$-b-PDMAEMA-b-$PMEO_2MA$ was also synthesized using ATRP[44]. MeO_2MA (5.82 mL), PMDETA (130 μL) and the macroinitiator Br-PDMAEMA-Br (2.7 g) dissolved in THF (20 mL) were placed in a 50-mL Schlenk flask. After three freeze–pump–thaw cycles, the catalyst CuBr (43.2 mg) was added to the degassed solution. The flask was immersed in an oil bath whose temperature was maintained at 40 °C for 10 h. The mixture was diluted with THF and passed through a neutral alumina column to remove residual CuBr. After the evaporation of excess THF, the mixture was precipitated in cold diethyl ether three times to remove unreacted monomers and other impurities. After drying under vacuum overnight, the block copolymer was collected and characterized.

Synthesis of PDMAEMA-b-$PMEO_2MA$-b-PDMAEMA. DMAEMA (3.7 mL), PMDETA (85 μL) and macroinitiator Br-$PMEO_2MA$-Br (2.5 g) dissolved in THF (12 mL) were placed in a 50-mL Schlenk flask. After three freeze–pump–thaw cycles, the catalyst CuBr (28.8 mg) was added into the degassed solution. The flask was immersed in an oil bath whose temperature was maintained at 40 °C for 10 h. The mixture was then diluted with THF and passed through a neutral alumina column to remove the residual CuBr. After evaporation of excess THF, the mixture was precipitated in cold n-hexane for three times to remove unreacted monomers and other impurities. After drying under vacuum overnight, the block copolymer was collected and characterized.

Synthesis of Citrate-Stabilized Gold Nanoparticles. All glassware was first washed with aqua regia and then rinsed with Milli-Q water several times prior to synthesis. Uniform 14-nm-diameter gold nanoparticles were prepared via the citrate reduction of $HAuCl_4$ in the aqueous phase. Typically, a sodium citrate water solution (2

mL, 51 mg/mL) was rapidly injected into a boiling $HAuCl_4$ (0.154 mL, 0.494 mol/L) aqueous solution under vigorous stirring. After boiling for 15 min, the solution was cooled to room temperature.

Polymer Coating of Gold Nanoparticles. The AuNPs were functionalized with $PMEO_2MA$-b-PDMAEMA-b-$PMEO_2MA$. To initiate the binding of the polymer to the surfaces of the Au nanoparticles, the disulfide linkage was reduced with tris(2-carboxyethyl) hydrochloride (TCEP)[26]. A total of 8 mg of TCEP was added to 20 mL of $PMEO_2MA$-b-PDMAEMA-b-$PMEO_2MA$ solution (5 mg/mL), and the mixture was then stirred for 30 min at room temperature after the pH was adjusted to 9-10. Next, the polymer solution was added dropwise to the concentrated AuNP solution via centrifugation at 0 °C. After being stirred at 0 °C overnight, the resulted conjugates were purified via centrifugation three times at 4 °C and 12000 r/min for 30 min. The final product was redispersed in pure water for the following experiments. The product named as Au@PDMAEMA-b-$PMEO_2MA$. The Au@$PMEO_2MA$-b-PDMAEMA NPs were prepared following a similar procedure by using PDMAEMA-b-$PMEO_2MA$-b-PDMAEMA.

Gel Permeation Chromatography (GPC). The molecular weight and polydispersity index (PDI) of the polymers were determined via gel permeation chromatography (GPC) using THF as the eluent at a flow rate of 1.0 mL min^{-1} at 25 °C and with narrow dispersed polystyrene (PS) as the calibration standard.

Proton Nuclear Magnetic Resonance Spectroscopy (^{1}H-NMR). A Bruker 300-MHz NMR spectrometer instrument was used to acquire the proton NMR spectra of the homopolymers and block copolymers using $CDCl_3$ as the solvent.

UV−Visible (UV−Vis) Spectrophotometry. The UV−Vis measurements were collected using a UV−Vis spectrophotometer (UV-2450, Shimadzu, Japan) between 200 nm and 700 nm using a cuvette with a 2-mm path length. The transmittance of the polymer solutions was monitored in a quartz cuvette (1 cm in width) as a function of the temperature at a wavelength of 520 nm. Heating and cooling scans were performed between 20 °C and 70 °C at a scanning rate of 0.1 °C/min.

Dynamic Light Scattering (DLS). Dynamic light scattering measurements were performed using a Zetasizer NanoZS Instrument (Malvern Instruments, UK) equipped with a 4-mW He−Ne laser (λ_0=633 nm) and with noninvasive backscattering (NIBS) detection at a scattering angle of 173°. The autocorrelation function was converted into a volume-weighted particle size distribution using Dispersion Technology Software 5.06 from

Malvern Instruments. Each measurement was repeated at least three times, and the average result was used as the final hydrodynamic diameter (Dh) distribution.

Transmission electron microscopy (TEM). Samples were prepared by depositing a drop of solution onto a holey carbon-coated Cu grid and allowing it to dry in air. The microstructure of the colloids was imaged using a transmission electron microscope (JEOL TEM-1400) operating at 100 kV.

Atomic Force Microscopy (AFM). The AFM topographic images were acquired using a Solver P47-PRO (NT-MDT Co., Moscow, Russia) microscope in tapping mode with a triangular microfabricated cantilever (Mikro Masch Co., Russia) with a length of 100 μm, a Si pyramidal tip, and a spring constant of 5.1 N m^{-1}. A resonance frequency in the range of 55-500 kHz was used, and resonance peaks in the frequency response of the cantilever typically located at 187 kHz were chosen for the tapping-mode oscillation. The measurements were performed under ambient conditions.

Supporting Information is available free of charge via the Internet at http://pubs.acs.org.

Conflict of Interest: The authors declare no competing financial interest.

ACKNOWLEDGMENTS

The authors gratefully acknowledge financial support from the National Natural Science Foundation of China (Nos. 21176065, 21376073, 91334203), the 111 Project of the Ministry of Education of China (No. B08021), and the Fundamental Research Funds for the Central Universities of China.

REFERENCES AND NOTES

1 J.-F. Gohy and Y. Zhao, Photo-responsive block copolymer micelles: design and behavior, *Chem. Soc. Rev.*, 2013, 42, 7117-7129.

2 P. Schattling, F. D. Jochum and P. Theato, Multi-stimuli responsive polymers – the all-in-one talents, *Polym. Chem.*, 2014, 5, 25-36.

3 J. Hu, G. Zhang, Z. Ge and S. Liu, Stimuli-responsive tertiary amine methacrylate-based block copolymers: Synthesis, supramolecular self-assembly and functional applications, *Prog. Polym. Sci.*, 2014, 39, 1096-1143.

4 E. G. Kelley, J. N. Albert, M. O. Sullivan and T. H. Epps III, Stimuli-responsive copolymer solution and surface assemblies for biomedical applications, *Chem. Soc. Rev.*, 2013, 42, 7057-7071.

5 S. Strandman and X. X. Zhu, Thermo-responsive block copolymers with multiple phase transition temperatures in aqueous solutions, *Prog. Polym. Sci.*, 2015, 42, 154-176.

6 G. Riess, Micellization of block copolymers, *Prog. Polym. Sci.*, 2003, 28, 1107-1170.

7 J. Weiss and A. Laschewsky, One-step synthesis of amphiphilic, double thermoresponsive diblock copolymers, *Macromolecules*, 2012, 45, 4158-4165.

8 J. Yun, R. Faust, L. S. Szilágyi, S. Kéki and M. Zsuga, Effect of Architecture on the Micellar Properties of Amphiphilic Block Copolymers: Comparison of AB Linear Diblock, A1A2B, and A2B Heteroarm Star Block Copolymers, *Macromolecules*, 2003, 36, 1717-1723.

9 M. A. Ward and T. K. Georgiou, Thermoresponsive triblock copolymers based on methacrylate monomers: effect of molecular weight and composition, *Soft Matter*, 2012, 8, 2737-2745.

10 M. A. Ward and T. K. Georgiou, Thermoresponsive terpolymers based on methacrylate monomers: Effect of architecture and composition, *J. Polym. Sci., Part A: Polym. Chem.*, 2010, 48, 775-783.

11 M. A. Ward and T. K. Georgiou, Multicompartment thermoresponsive gels: does the length of the hydrophobic side group matter? *Polym. Chem.*, 2013, 4, 1893-1902.

12 X. Zhao, W. Liu, D. Chen, X. Lin and W. W. Lu, Effect of Block Order of ABA- and BAB- Type NIPAAm/HEMA Triblock Copolymers on Thermoresponsive Behavior of Solutions, *Macromol. Chem. Phys.*, 2007, 208, 1773-1781.

13 T. B. Bonné, K. Lüdtke, R. Jordan and C. M. Papadakis, Effect of Polymer Architecture of Amphiphilic Poly (2-oxazoline) Copolymers on the Aggregation and Aggregate Structure, *Macromol. Chem. Phys.*, 2007, 208, 1402-1408.

14 J. Shan and H. Tenhu, Recent advances in polymer protected gold nanoparticles: synthesis, properties and applications, *Chem. Commun.*, 2007, 4580-4598.

15 D. Li, Q. He and J. Li, Smart core/shell nanocomposites: intelligent polymers modified gold nanoparticles, *Adv. Colloid Interface Sci.*, 2009, 149, 28-38.

16 C. Boyer, M. R. Whittaker, M. Luzon and T. P. Davis, Design and synthesis of dual thermoresponsive and antifouling hybrid polymer/gold nanoparticles, *Macromolecules*, 2009, 42, 6917-6926.

17 M. Karg, N. Schelero, C. Oppel, M. Gradzielski, T. Hellweg and R. von Klitzing, R. Versatile phase transfer of gold nanoparticles from aqueous media to different organic media, *Chem. Eur. J.*, 2011, 17, 4648-4654.

18 A. Housni and Y. Zhao, Gold nanoparticles functionalized with block copolymers displaying either LCST or UCST thermosensitivity in aqueous solution, *Langmuir*, 2010, 26, 12933-12939.

19 J. Chen, P. Xiao, J. Gu, D. Han, J. Zhang, A. Sun, W. Wang and T. Chen, A smart hybrid system of Au nanoparticle immobilized PDMAEMA brushes for thermally adjustable catalysis, *Chem. Commun.*, 2014, 50, 1212-1214.

20 D. Li, C. Li, Y. Yang, Q. He and J. Li, Interfacial dispersion of poly (N-isopropylacrylamide)/gold nanocomposites, *J. Nanosci. Nanotechnol.*, 2011, 11, 2052-2056.

21 Z. Zhang, S. Maji, A. B. d. F. Antunes, R. De Rycke, Q. Zhang, R. Hoogenboom and B. G. De Geest, Salt plays a pivotal role in the temperature-responsive aggregation and layer-by-layer assembly of polymer-decorated gold nanoparticles, *Chem. Mater.*, 2013, 25, 4297-4303.

22 D. Li, Q. He, Y. Cui and J. Li, Fabrication of pH-responsive nanocomposites of gold nanoparticles/poly (4-vinylpyridine), *Chem. Mater.*, 2007, 19, 412-417.

23 E. W. Edwards, M. Chanana and D. Wang, Capping Gold Nanoparticles with Stimuli-responsive Polymers to Cross Water−Oil Interfaces: In-Depth Insight to the Trans-Interfacial Activity of Nanoparticles, *J. Phys. Chem. C*, 2008, 112, 15207-15219.

24 A. Barhoumi, W. Wang, D. Zurakowski, R. S. Langer and D. S. Kohane, Photothermally Targeted Thermosensitive Polymer-Masked Nanoparticles, *Nano Lett.*, 2014, 14, 3697-3701.

25 M. S. Strozyk, M. Chanana, I. Pastoriza□Santos, J. Pérez-Juste and L. M. Liz-Marzán, Protein/Polymer-Based Dual-Responsive Gold Nanoparticles with pH-Dependent Thermal Sensitivity, *Adv. Funct. Mater.*, 2012, 22, 1436-1444.

26 K. L. Hamner and M. M. Maye, Thermal Aggregation Properties of Nanoparticles Modified with Temperature Sensitive Copolymers, *Langmuir*, 2013, 29, 15217-15223.

27 L. Cheng, A. Liu, S. Peng and H. Duan, Responsive Plasmonic Assemblies of Amphiphilic Nanocrystals at Oil− Water Interfaces, *ACS Nano*, 2010, 4, 6098-6104.

28 J. M. Horton, C. Bao, Z. Bai, T. P. Lodge and B. Zhao, Temperature-and pH-triggered reversible transfer of doubly responsive hairy particles between water and a hydrophobic ionic liquid, *Langmuir*, 2011, 27, 13324-13334.

29 A. Stocco, M. Chanana, G. Su, P. Cernoch, B. P. Binks and D. Wang, Bidirectional Nanoparticle Crossing of Oil–Water Interfaces Induced by Different Stimuli: Insight into Phase Transfer, *Angew. Chem., Int. Ed.*, 2012, 51, 9647-9651.

30 Y. Song and S. Chen, Janus Nanoparticles as Versatile Phase-Transfer Reagents, *Langmuir*, 2014, 30, 6389-6397.

31 Y. Shi, V. Selin, Y. Wang and S. A. Sukhishvili, Multiresponsive Block Copolymer-Modified "Hairy" Gold Nanoparticles for Remote Control of Interfaces, *Part. Part. Syst. Charact.*, 2013, 30, 950-957.

32 J. He, Y. Liu, T. Babu, Z. Wei and Z. Nie, Self-assembly of inorganic nanoparticle vesicles and tubules driven by tethered linear block copolymers, *J. Am. Chem. Soc.*, 2012, 134, 11342-11345.

33 J. Dong, J. Li and J. Zhou, Interfacial and phase transfer behaviors of polymer brush grafted amphiphilic nanoparticles: a computer simulation study, *Langmuir*, 2014, 30, 5599-5608.

34 J. Dong and J. Zhou, Solvent-Responsive Behavior of Polymer-Brush-Modified Amphiphilic Gold Nanoparticles, *Macromol. Theory Simul.*, 2013, 22, 174-186.

35 S. Volden, J. L. Eilertsen, G. Singh, W. Wang, K. Zhu, B. Nyström and W. R. Glomm, Effect of Charge Density Matching on the Temperature Response of PNIPAAM Block Copolymer–Gold Nanoparticles, *J. Phys. Chem. C*, 2012, 116, 12844-12853.

36 B. Y. Zhang, W. D. He, W. T. Li, L. Y. Li, K. R. Zhang, H. Zhang. Preparation of block-brush PEG-b-P(NIPAM-g-DMAEMA) and its dual stimulus-response. *Polymer*, 2010, 51, 3039-3046.

37 G. Liu, D. Wu, C. Ma, G. Zhang, H. Wang, S. Yang, Insight into the Origin of the Thermosensitivity of Poly[2-(dimethylamino)ethyl methacrylate]. *ChemPhysChem*, 2007, 8, 2254 – 2259.

38 A. Car, P. Baumann, J. T. Duskey, M. Chami, N. Bruns, W Meier. pH-Responsive PDMS-b-PDMAEMA Micelles for Intracellular Anticancer Drug Delivery. *Biomacromolecules*, 2014, 15, 3235-3245.

39 Y. Zhang, J. L. He, D. L. Cao, M. Z. Zhang, P. H. Ni. Galactosylated reduction and pH dual-responsive triblock terpolymer Gal-PEEP-a-PCL-ss-PDMAEMA: a multifunctional carrier for the targeted and simultaneous delivery of doxorubicin and DNA. *Polymer Chemistry*, 2014, 5, 5124-5138.

40 M. Wagner, C. Pietsch, A. Kerth, A. Traeger, U. S. Schubert, Physicochemical Characterization of the Thermo-Induced Self-Assembly of Thermo-Responsive PDMAEMA-b-PDEGMA Copolymers. *J. Polym. Sci. Part A-Polym. Chem.*, 2015, 53, 924-935.

41 A. P. Filippov, E. V. Belyaeva, N. V. Zakharova, A. S. Sasina, D. M. Ilgach, T. K. Meleshko, A. V. Yakimansky. Double stimuli-responsive behavior of graft copolymer with polyimide backbone and poly(N,N-dimethylaminoethyl methacrylate) side chains. *Colloid Polym. Sci.*, 2015, 293, 555-565.

42 E. W. Edwards, M. Chanana, D. Wang and H. Möhwald, Stimuli-Responsive Reversible Transport of Nanoparticles Across Water/Oil Interfaces, *Angew. Chem., Int. Ed.*,2008, 47, 320-323.

43 K. Zhou, Y. Wang, X. Huang, K. Luby-Phelps, B. D. Sumer and J. Gao, Tunable, Ultrasensitive pH-Responsive Nanoparticles Targeting Specific Endocytic Organelles in Living Cells, *Angew. Chem., Int. Ed.*, 2011, 50, 6109-6114.

44 X. Han, X. Zhang, H. Zhu, Q. Yin, H. Liu and Y. Hu, Effect of composition of PDMAEMA-b-PAA block copolymers on their pH-and temperature-responsive behaviors, *Langmuir*, 2013, 29, 1024-1034.